IOP Publishing | Journal of Physics D: Applied Physics
J. Phys. D: Appl. Phys. **50** (2017) 025304 (8pp) | doi:10.1088/1361-6463/50/2/025304

Dynamic behavior of a black phosphorus and carbon nanotube composite system

Jiao Shi[1], Haifang Cai[1], Kun Cai[1,2] and Qing-Hua Qin[2]

[1] College of Water Resources and Architectural Engineering, Northwest A&F University, Yangling 712100, People's Republic of China
[2] Research School of Engineering, the Australian National University, ACT 2601, Australia

E-mail: kuncai99@163.com and qinghua.qin@anu.edu.au

Received 26 September 2016, revised 23 October 2016
Accepted for publication 31 October 2016
Published 1 December 2016

Abstract

A double walled nanotube composite is constructed by placing a black-phosphorene-based nanotube (BPNT) in a carbon nanotube (CNT). When driving the CNT to rotate by stators in a thermal driven rotary nanomotor, the BPNT behaves differently from the CNT. For instance, the BPNT can be actuated to rotate by the CNT, but its rotational acceleration differs from that of the CNT. The BPNT oscillates along the tube axis when it is longer than the CNT. The results obtained indicate that the BPNT functions with high structural stability when acting as a rotor with rotational frequency of ~20 GHz at 250 K. If at a higher temperature than 250 K, say 300 K, the rotating BPNT shows weaker structural stability than its status at 250 K. When the two tubes in the rotor are of equal length, the rotational frequency of the BPNT drops rapidly after the BPNT is collapsed, owing to more broken P–P bonds. When the black-phosphorene nanotube is longer than the CNT, it rotates synchronously with the CNT even if it is collapsed. Hence, in the design of a nanomotor with a rotor from BPNT, the working rotational frequency should be lower than a certain threshold at a higher temperature.

Keywords: nanomotor, nanotube, black phosphorus, molecular dynamics

S Online supplementary data available from stacks.iop.org/JPhysD/50/025304/mmedia

(Some figures may appear in colour only in the online journal)

1. Introduction

Few-layered black phosphorus has become a new wonder among 2D materials [1–6] due to its excellent semi-conducting and photovoltaic properties [7–15]. Similar to CNTs [16–22] imaged from a curved graphene ribbon along a direction [1, 23–26], black phosphorus nanotubes (BPNTs) can also be considered a product of a curved black phosphorene ribbon. Over the past two decades, much research has been conducted on the electrical properties of such nanotubes [27, 28]. It is wellknown that phosphorus has many allotropes, which can be transformed from one to another under certain temperature and compression [29–31]. The existence of such phosphorus allotropes makes the structural stability of black phosphorus lower than that of graphene. This phenomenon can be attributed to the electron structure of such material. For example, in a graphene ribbon, the carbon atoms are covalently bonded with $2sp^2$ electrons, which provide high bond energy and lead to the relatively high stiffness and strength of the graphene [32–34]. In black phosphorene, however, the phosphorus–phosphorus (P–P) bond is formed with $3sp^3$ electrons. The distance between the two nuclei is ~0.24 nm, far greater than that between any two bonded atoms in graphene (~0.142 nm). Hence, black phosphorene has lower modulus and strength than graphene [35–37]. Based on this understanding, Cai *et al* [38, 39] thought the structural stability of BPNT could be maintained before the tube worked as a component of a nanodevice. They first discussed the thermal stability of BPNT at finite temperature, and proposed the critical curvature of BPNTs at different temperatures. For example, for a BPNT formed by curling a rectangular black phosphorene ribbon along the armchair (pucker) direction (see figures 1(a) and (b)), the minimal number of periodic unit cells (figure 1(c)) should be 16 at 300 K. If curved along a zigzag direction

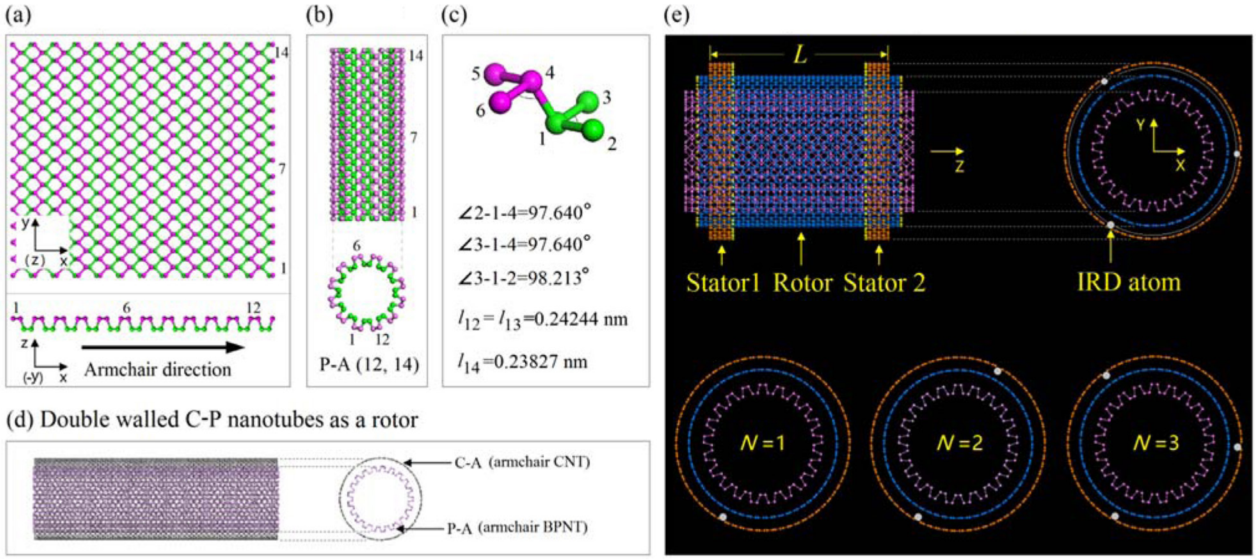

Figure 1. Geometric model of a thermally driven rotary nanomotor with two stators made from CNT and a rotor made from composite double-walled carbon–phosphorus (CP) nanotubes. Each outer end of stators has N carbon atoms with the same inward radial deviation (IRD). N is 1, 2, or 3 in the present study. The value of IRD is 0.3 times the sp^2 C–C bond length (i.e. 0.142 nm). Each carbon atom at the inner ends of stators or at both ends of the mid tube (C–A) is bonded with a hydrogen atom. The axial distance between the adjacent outer ends of rotor and a stator is 0.246 nm. The axial length of BPNT is 5.965 nm. When $L = 5.362$ nm, the axial length of two tubes in rotor can be considered **equal**. When $L = 4.870$ nm (current model in (e)), the axial lengths of the two tubes inrotor are **unequal**. Detailed information on the model is given in table 1. 'n_A' of the BPNT, the number of unit cells along the armchair direction, is 12 in schematic (b), but in (e) for simulation, it is 21. (a) Black phosphorene (BP). (b) BPNT. (c) Unit cell of BP. (d) Double walled C–P nanotubes as a rotor. (e) Thermally driven rotary nanomotor.

Table 1. Geometrical parameters of nanotubes in the thermally driven rotary nanomotor.

Component	Tube type	Chirality	Number of atoms	Tube length/nm	Diameter/nm
Inner tube	P–A	(**21**, 18)	1554 P	5.965	2.93
Mid tube (**Equal**)	C–A	(29, 29)	2726 C + 116 H	5.854	3.93
Mid tube (**Unequal**)	C–A	(29, 29)	2494 C + 116 H	5.362	3.93
Outer tubes	C–A	(34, 34)	2 × (340 C + 68 H)	2 × 0.492	4.61

(in-plane but normal to the armchair direction), the minimal number should be 52 at 300 K. In general, the minimal number increases with the increase of temperature. Further, they discussed the damage and buckling behavior of a BPNT under axial compression at finite temperatures. It was found that buckling of the tube was followed by fracturing.

As reported in work by Guo *et al* [28], a BPNT is semiconductor with direct bandgap. Now, assuming a nanomachine that requires BPNTs as its semiconductor components, the dynamic behavior of the BPNT-based components is essential for some special functions of the nanomachine. As the structure of BPNT intuitively has weak stability [38, 39], the components should be protected by high strength nanotubes such as CNTs. Consequently, the typical question may be asked: if a BPNT is used in a high-speed rotary nanomotor [40–44], how can we ensure a stable system during rotation? To address this issue, the dynamic behavior of a BPNT in a CNT with high rotational frequency is investigated in the present study. To induce the rotation of a CNT that contains a BPNT (figure 1(d)), we adopt thermally driven rotary nanomotor in simulation. The mechanism can be explained briefly thus: the collision between rotor and stator(s) is produced by the thermal vibration of the atoms on the tubes. When one or more carbon atoms at the end of stator(s) have inward radial deviation (IRD), the stator will exert a circumferential moment on the rotor during collision. The rotor will be driven to rotate by the circumferential moment [44]. In this study, the influence of major factors such as temperature, rotational acceleration, and centrifugal effect on the dynamic behavior of the BPNT are demonstrated.

2. Models and methodology

In the system, there are three types of elements, phosphorus, carbon, and hydrogen. The interaction among the atoms is illustrated with three different potential functions. For example, the interaction among phosphorous atoms, the Stillinger–Weber [45] potential with new parameters developed by Jiang [46], is adopted. The interaction among carbon and hydrogen atoms will be described by the adaptive intermolecular reactive empirical bond order (AIREBO) potential [47]. The interaction between phosphorus and carbon atoms is evaluated through a 12-6 Lennard-Jones potential [48], $V(r) = 4\varepsilon_{C\text{–}P}[(\sigma_{C\text{–}P}/r)^{12} - (\sigma_{C\text{–}P}/r)^{6}]$, with constants of $\varepsilon_{C\text{–}P} = 6.878 \times 10^{-3}$ eV and $\sigma_{C\text{–}P} = 0.342\,25$ nm. The cutoff distance is 1.0 nm. The 12-6 Lennard-Jones potential for neighboring carbon/hydrogen atoms has constants of $\varepsilon_{C\text{–}C} = 2.84 \times 10^{-3}$ eV and $\sigma_{C\text{–}C} = 0.34$ nm, or $\varepsilon_{H\text{–}H} = 1.50 \times 10^{-3}$ eV and $\sigma_{H\text{–}H} = 0.265$ nm, or

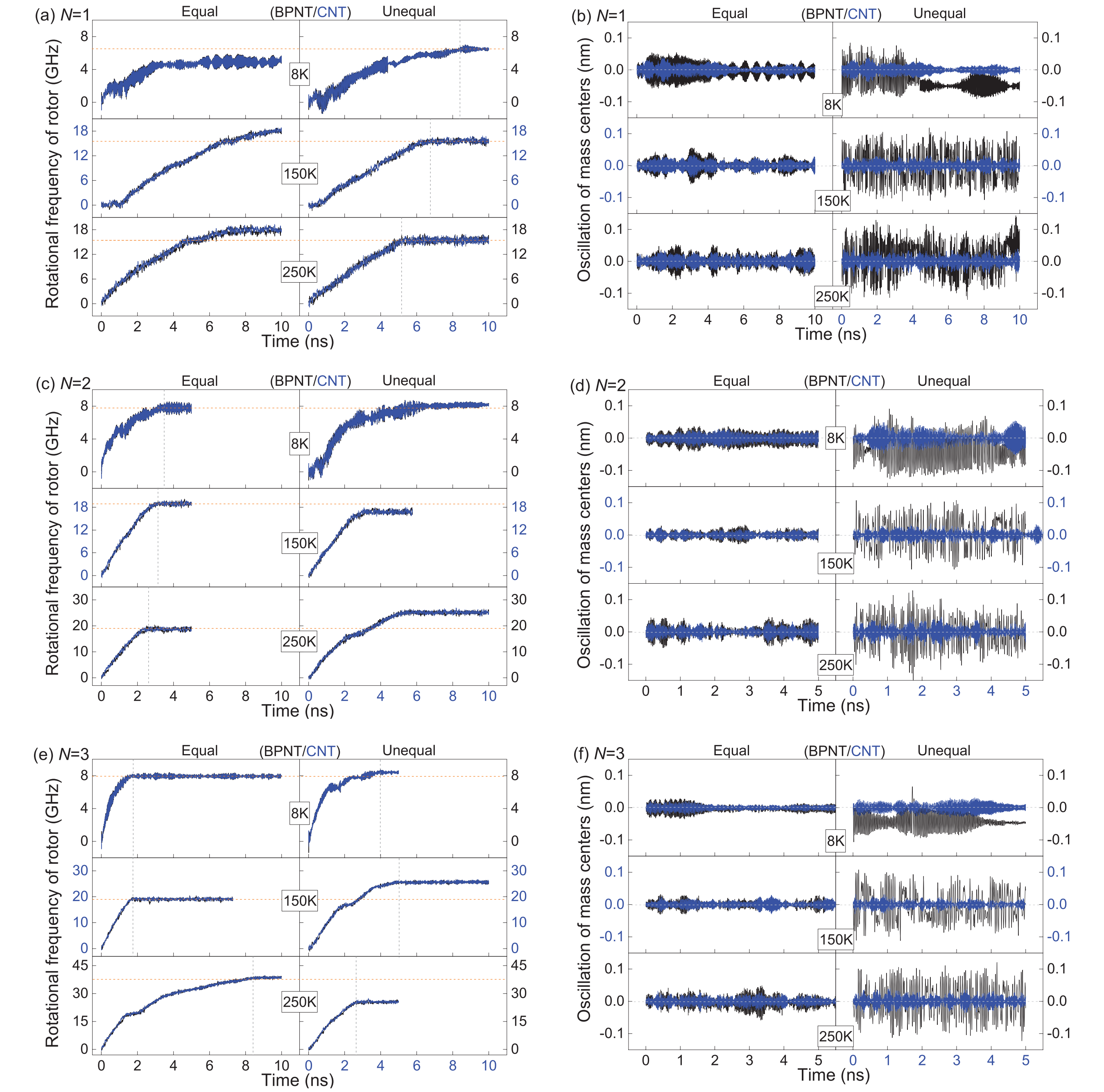

Figure 2. Rotation and oscillation of BPNT and CNT in rotor, which is driven by stators with different IRD atoms and at different temperature. (a) and (b) $N = 1$. (c) and (d) $N = 2$. (e) and (f) $N = 3$.

$\varepsilon_{C\text{–}H} = 1.376 \times 10^{-3}$ eV and $\sigma_{C\text{–}H} = 0.3025$ nm, respectively. The interaction between phosphorus and hydrogen atoms is neglected.

For studying the rotational behavior of the composite double-walled nanotubes (DWNTs) driven by the CNT-based stators in a canonical NVT ensemble, five steps are operated:

(1) Build a rotor from CP DWNTswith specified geometry (figure 1(d));
(2) Create a thermally driven rotary nanomotor from the rotor in Step (1) and CNT-based stators with specified IRD atoms;
(3) Carry out energy minimization of the whole system by the steepest descent algorithmwith tolerance on energy and force relative error of 10^{-4} and 10^{-6}, respectively;
(4) Fix all carbon atoms on the stators with their degrees of freedom, and place the rest atoms in a canonical NVT ensemble using Nosé–Hoover thermostat [49];
(5) Write down the necessary data, e.g. rotational frequency, rotor's mass center, for post-processing during 5–10 ns of running.

Open source code LAMMPS [50, 51] is used to simulate the behaviors of the rotor with the time step of 1.0 fs. To show the temperature effect on the dynamic behavior of the rotor,

Table 2. Stable rotational frequencies of tubes in rotor. The statistics is calculated during (9.501, 10.000) ns or (4.501, 5.000) ns. The difference of rotational frequency is relative to that of CNT.

		$N = 1$			$N = 2$			$N = 3$		
Scheme		$T = 8$ K	150 K	250 K	$T = 8$ K	150 K	250 K	$T = 8$ K	150 K	250 K
Equal	BPNT	5.033	18.011	17.680	7.769	19.019	18.730	7.937	19.022	31.670
	CNT	5.040	18.102	18.004	7.778	18.960	18.749	7.934	19.086	31.694
	Difference	0.007	0.091	0.324	0.009	−0.059	0.019	0.003	0.064	0.024
Unequal	BPNT	6.476	15.397	15.697	8.175	16.793	25.239	8.399	25.524	25.726
	CNT	6.473	15.660	15.436	8.177	16.812	25.072	8.397	25.617	25.486
	Difference	−0.003	0.264	−0.261	0.002	0.019	−0.167	−0.002	0.093	−0.240

three temperatures are used, separately, i.e. 8 K, 150 K, and 300 K. In the present study, the temperature is estimated using the total kinetic energy of atoms on the rotor according to the state equation $E_{\mathrm{Kinetic}} = \frac{3}{2}kT$, where E_{Kinetic} represents the sum of the average kinetic energy of all the atoms in the system, k is the Bolzmann constant, T is temperature.

3. Results and discussion

3.1. Rotation and oscillation of tubes in rotor

According to the theory of thermally driven rotary nanomotors proposed by Cai *et al* [42–44], the rotor in figure 1(e) will be actuated to rotate on the condition that the number of N is no less than 1 and the system is an open system, e.g. in a canonical NVT ensemble. With or without the presence of BPNT, the CNT in the rotor will be accelerated to rotate as time progresses. However, when the torque moment provided by two stators on the CNT in the rotor is a constant, the acceleration of the rotor without BPNT must be greater than that of the rotor made from composite CP nanotubes by virtue of having lower moment of inertia along the z-axis. With the presence of BPNT, the rotational acceleration depends on both the interaction between the CNT in the rotor and that between the two tubes in the rotor. According to Newton's Third Law of Motion, that the mutual forces of action and reaction between two particles/rigid bodies are equal, opposite and collinear, the rotation of the BPNT will also be excited by the CNT in rotor. The mutual forces are well-known frictional forces between two tubes in a rotor due to their relative motion. The circular component of frictional force can be estimated using the equation:

$$F_{\mathrm{Fric}} \approx \frac{1}{\bar{r}} \frac{\Delta\omega}{\Delta t} \sum_i m_i \cdot r_i^2 \tag{1}$$

where $\bar{r}$ is the average radius of BPNT and CNT, F_i is the frictional force exerted on the ith atom on the BPNT, r_i is the relative distance from the atom to the rotary axis of the BPNT. ω is the angular velocity of the tube, as shown in figures 2 and 3, and t means time.

From figure 2(a), we find that the two tubes in the rotor have almost the same historical curve of rotation. At 8 K, the final stable rotational frequency of the rotor with two tubes of unequal length, i.e. ~6.5 GHz (see table 2), is higher than that of the rotor with two tubes of equal length (~5.0 GHz). But the converse is true at higher temperature, e.g. 150 K or 300 K. From comparisons of figures 2(a), (c) and (e), two conclusions can be drawn for the rotor with two tubes of equal length. The first is that the same rotor driven by the same stator has a higher rotational speed at higher temperatures. The second conclusion is that the final stable rotational frequency of a rotor is higher if it has the same geometry at the same temperature but is driven by stators with more IRD atoms, i.e. N is higher. When the two tubes in a rotor are of unequal length, the second conclusion becomes uncertain. The reason is that the interaction between the ends of BPNT and CNT in the rotor [52] becomes unstable during rotation (movie 1) (stacks.iop.org/JPhysD/50/025304/mmedia). This can be revealed from the results shown in figures 2(b), (d) and (f). For example, when the lengths of two tubes are equal, the axial oscillation of the two tubes remains almost synchronous. However, if the two tubes are of different lengths, the oscillation of the BPNT (black curve) has a higher amplitude than that of the CNT (blue curve),or the right ends of BPNT and CNT are finally aligned (see the curve $N = 1$/unequal/at 8 K, or $N = 3$/unequal/at 8 K).

Besides the relative sliding along the z-axis between BPNT and CNT in the rotor, the two tubes actually undergo circumferential sliding during rotation. As we enlarge the curve in figures 2(c) and (e) during (1.0, 1.3) ns, i.e. figure 3, the two curves in each inserted subfigure fluctuate alternately. A curve with an upward tendency implies that the tube has positive acceleration of rotation. Similarly, a downward tendency represents negative acceleration. Hence, the curves in figure 3 demonstrate the friction between the two tubes in the rotor. Besides, the absolute values of acceleration of the two curves at the same moment are different because the two tubes in the rotor have different moments of inertia and different torque moments. Even when the rotational frequencies of rotorsare averaged over time, the two tubes also have different acceleration of rotation (see table 3). But the difference is so slight that it leads to the alignment of the two curves in each subfigure in figures 2(a), (c) and (e). By accumulating the rotational speed over a long period of time, the relative sliding between BPNT and CNT can be found clearly. For example, figure 4 gives the rotational angle of two tubes in a rotor when $N = 3$, BPNT and CNT are of equal length, and at a temperature of 250 K. From the figure, we find that the relative rotation of BPNT and CNT becomes obvious after about 0.22 ns, and becomes more obvious after 1.1 ns. In

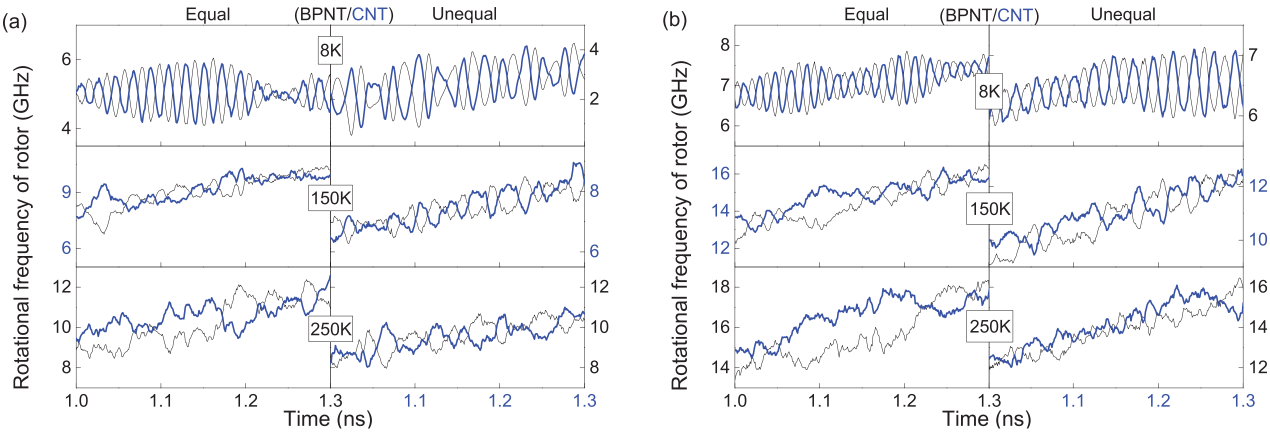

Figure 3. Difference between rotational history curves of BPNT and CNT in rotor:(a) when $N = 2$; (b) when $N = 3$.

Table 3. Over a specified duration, the average rotational acceleration of BPNT in rotor at different conditions. (Unit: $2\pi \times 10^9$ rad s^{-2}).

	$N = 1$			$N = 2$			$N = 3$		
Scheme	8 K	150 K	250 K	8 K	150 K	250 K	8 K	150 K	250 K
Equal	1.41	2.42	2.70	1.75	6.56	7.89	5.28	11.62	12.16
Unequal	1.48	2.58	2.67	3.64	6.16	6.85	5.39	10.32	12.09
Duration/ns	(1.0, 3.0)	(2.0, 5.0)	(1.0, 4.0)	(0.5, 2.0)	(0.5, 2.0)	(0.5, 2.0)	(0.2, 1.0)	(0.2, 1.5)	(0.2, 1.5)

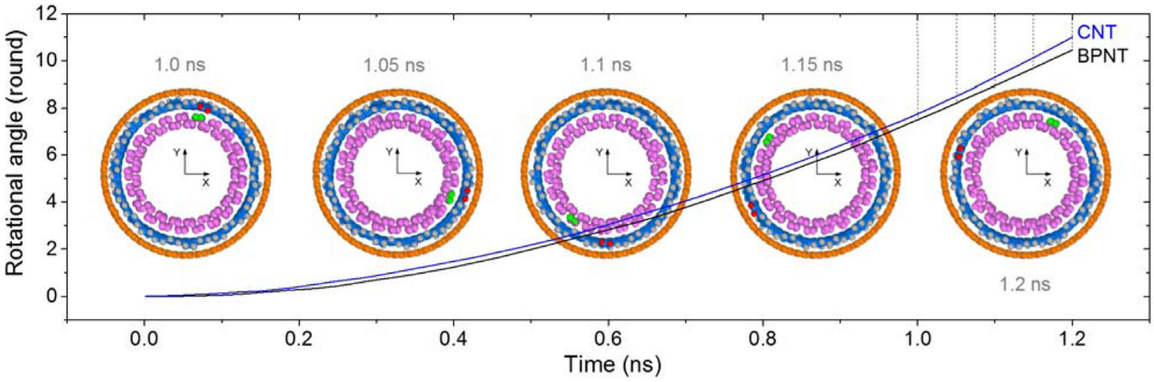

Figure 4. Rotation of tubes in rotor when $N = 3$ and the two tubes in the rotor are of **equal** length at 250 K. The tubes in the rotor have anticlockwise rotation. To reveal the relative rotation, two green atoms and two red atoms are labeled on the BPNT and CNT, respectively, from 1.0 ns to 1.2 ns.

particular, five representative snapshots of the system have been inserted in the figure. We find that the relative rotational angle between the two tubes in the rotor, i.e. the relative positions of the green atoms on BPNT and the red atoms on CNT, is over 60° from 1.0 ns to 1.2 ns (movie 2). Hence, in present model, the two tubes do not rotate synchronously. Moreover, the relative rotational angle becomes higher over a longer period of time, as can be verified by the data in table 4. But the growth rate of the relative rotational angle decreases because the rotational frequencies of two tubes tendto be stable. For instance, over (1.5, 2.0) ns, the relative rotational angle grows 0.08(=0.71 − 0.63) cycle. Over (2.5, 3.0) ns, the angle increases by 0.05 (=0.92 − 0.87) cycle. Over (4.5, 5.0) ns, it increases only 0.02 cycle. Therefore, we can conclude that the growth ratio tends to be zero within a few nanoseconds. That means that the two tubes, BPNT and CNT, in the rotor will rotate synchronously, a reasonable conclusion because the circumferential friction between BPNT and CNT leads to dissipation of kinetic energy. As the CNT approaches a stable state, e.g. stable rotation, the rotation of BPNT increases more slowly than during the initial stage. When the two tubes have identical rotational frequency, the system reaches a stable state. It is not possible for the rotational frequency of the BPNT to remain higher than that of the CNT over a long duration, because the intertube friction leads to a decreasein the rotation of the BPNT.

3.2. Collapse of BPNT during rotation

The structure of BPNT remains stable during rotation in each case of figure 2, demonstrating that the BPNT can act as a rotary nanodevice at low temperature, e.g. no more than

Table 4. Rotational angle of tubes in rotor when $N = 3$ and the two tubes in the rotor are of **equal** length at 250 K. (Unit: one rotation).

Time/ns	0.0	0.5	1.0	1.5	2.0	2.5	3.0	3.5	4.0	4.5	5.0
CNT	0	2.18	7.76	16.47	26.07	36.57	48.78	62.47	78.19	92.50	108.35
BPNT	0	1.98	7.50	15.84	25.36	35.70	47.86	61.53	77.15	91.53	107.36
Difference	0	0.20	0.26	0.63	0.71	0.87	0.92	0.94	0.96	0.97	0.99

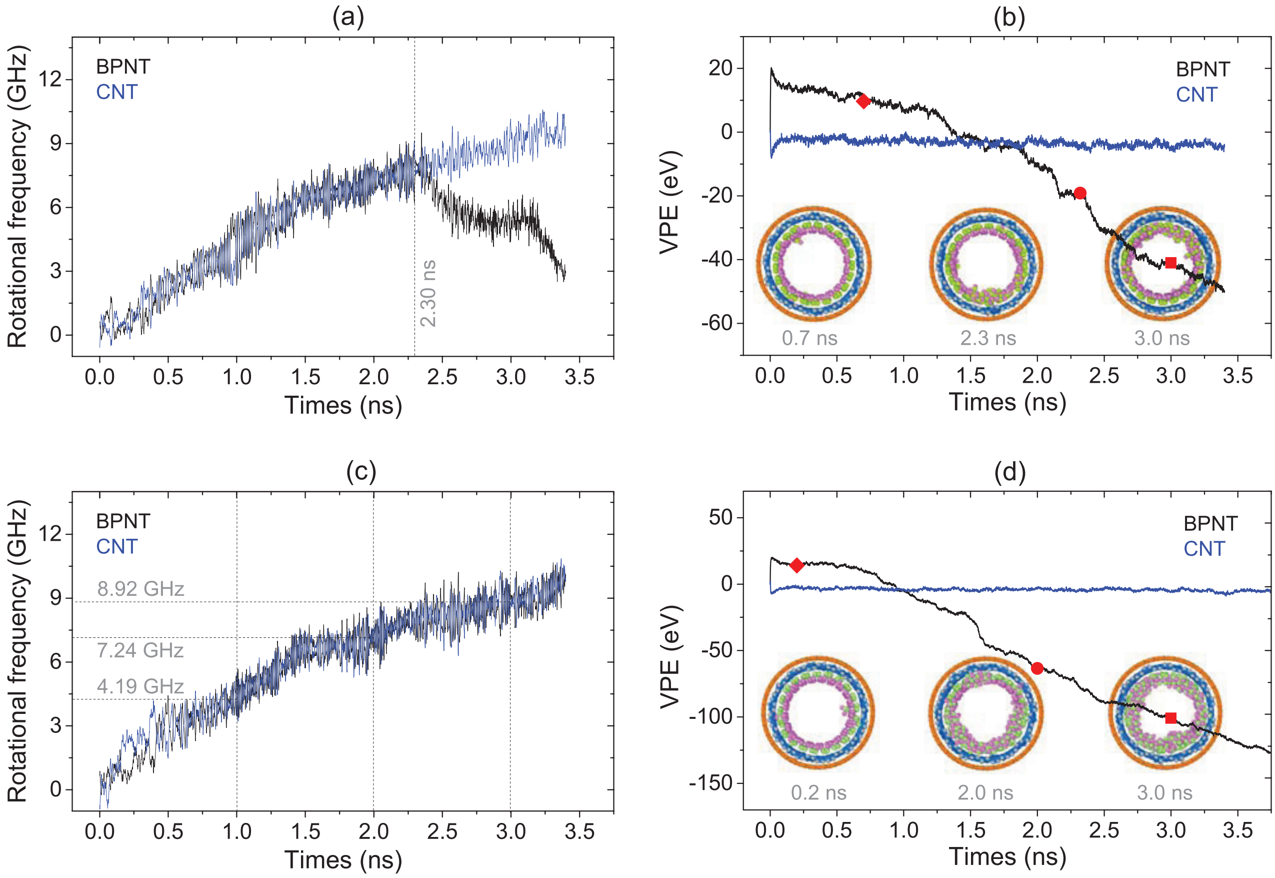

Figure 5. History curves of rotational frequency and variation of potential energy (VPE) of tubes in rotor when $N = 1$ at 250 K. (a) Rotation (equal). (b) Potential (equal). (c) Rotation (unequal). (d) Potential (unequal).

250 K. If temperature is higher, e.g. 300 K, how does the BPNT behave in the rotating CNT?

Relevant results [38] show that the structural stability of BPNT depends strongly on temperature. For example, the minimal number of periodic unit cells along the circumferential direction of a P–A BPNT is 16 at 300 K. Moreover, the BPNT should be free of constraints on degree of freedom. In the present model, the number, n_A, is 21 (see table 1) and the BPNT is protected by the CNT. Hence, at 300 K, the P–A (21, 18) BPNT is stable if there is no rotation. However, it is damaged soon after it is actuated to rotate at even few gigahertz of rotational frequency. The results in figure 5 show that the BPNT is severely damaged after 2.0 ns. When the BPNT is totally covered by the CNT, i.e. the two tubes are of equal length, a pair of phosphorus atoms at the end of the tube have left their original position at an earlier stage, e.g. 0.7 ns (figure 5(b)). After 2.3 ns of running, the BPNT is severely broken (movie 3). From figure 5(b), the potential energy drops continuously due to the interaction among phosphorous atoms varying to maintain stability of all the BPNT atoms within the CNT. From figure 5(a), we find that the two ‘tubes’ in the rotor have different rotational accelerations after 2.3 ns; that is, the CNT has positive acceleration whereas the BPNT has negative acceleration. This finding implies that the phosphorus atoms slide within the CNT that has a high rotational speed. Therefore, when the temperature is relatively high, the BPNT is not stable even when protected by the CNT. That is because the P–P bonds become longer than that at 0 K when the system is at higher temperature, and the strength of P–P bonds is reduced. At the same time, the vibration of carbon atoms on the CNT also influences the phosphorus atoms. Although the BPNT is protected by the CNT on its external surface, the phosphorus atoms can move inward. Hence, some atoms on the BPNT leave their position and move into the central area during the damage process.

As the two tubes in the rotor are of unequal length, the BPNT breaks earlier than in the ‘equal’ case. From figure 5(d), we find that the end P–P bonds have broken at 0.2 ns, that is, sooner than the 0.7 ns in figure 5(b). The VPE curve of the BPNT drops continuously, indicating that more and more P–P bonds break (movie 4). This conclusion can be verified by the differences in the three inserted configurations in figure 5(d).

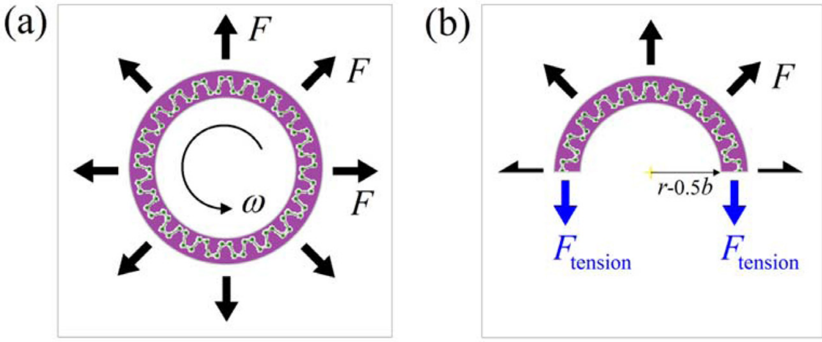

Figure 6. Internal tension due to rotational centrifugal force. (a) Uniform centrifugal load (F) on the circular ring with width b and averaged radius r. ω is the rotational frequency of the ring along the normal of ring. (b) Equilibrium state of a half-ring considering the internal tension force, F_{tension}.

Comparing these three configurations with those in figure 5(b), we find that some phosphorus atoms are attracted by the end carbon atoms on the CNT, indicating that the interaction between the two tubes in the rotor is greater than that between the BPNT and CNT of equal length. That is the reason why the two tubes rotate synchronously, as can be seen from figure 5(c), even though the BPNT is severely damaged. The phosphorus atoms attracted by the ends of CNT do not come closer to the tube axis because they are also under centrifugal force during rotation. From figure 5(c), the rotational frequency of rotor is over 7 GHz after 2.0 ns. Moreover, the mass of a phosphorus atom ($m_{\rm P}$) is about 3 times that of a carbon atom. Hence, the centrifugal effect on the motion of the phosphorus atoms is obvious and can be estimated using the equation

$$F_{\rm P} = m_{\rm P} \cdot r \cdot (2\pi\omega)^2 \tag{2}$$

where ω is the rotational frequency of BPNT, r is the distance between the phosphorus atom and the tube axis (figure 6). Therefore the average tension along the circumferential direction on the BPNT can be estimated as

$$\int_0^{\pi} F_{\rm P} \cdot \sin\theta \cdot r\mathrm{d}\theta - 2b \cdot F_{\text{tension}} = 0 \tag{3}$$

Considering the particle system (figure 1(e)), the average tension between two neighboring phosphorus atoms on the same cross-section of the BPNT can be expressed as

$$F_{\text{tension}} \approx \frac{r}{2b}\sum_{i=1}^{4\times n_{\rm A}/2} F_{\rm P}^{(i)} \sin\left(\frac{\pi \cdot i}{4\times n_{\rm A}/2}\right) = \frac{r}{2b}\sum_{i=1}^{42} F_{\rm P}^{(i)} \sin\left(\frac{\pi \cdot i}{42}\right) \tag{4}$$

Substituting equation (2) into equation (4), the critical rotational frequency with respect to the critical value of F_{tension} can be written as

$$\omega^{Crit} = \frac{1}{2\pi}\sqrt{\frac{F_{\text{tension}}^{\text{Crit}}}{\frac{m_{\rm P} r^2}{2b}\sum_{i=1}^{42}\sin\left(\frac{\pi \cdot i}{42}\right)}} \tag{5}$$

At a higher temperature, the critical value of F_{tension} is lower, leading to a lower value of the rotational frequency of the BPNT. This is essential for the BPNT with a greater length than the CNT.

4. Conclusions

The composite nanotube system with double walled nanotubes formed by putting a BPNT in a CNT is found to have unique dynamic behavior when the CNT is driven to rotate. By systematic discussion along with numerical experiments, some conclusions on the behavior of the composite rotorare drawn from the numerical experiments:

(1) At the same temperature, the final stable rotational frequency of the rotor is higher if the rotor is driven by stators with more IRD atoms, namely a higher value of N;
(2) During the acceleration period of the rotor, the friction between the BPNT and the CNT can be observed through differences in the history curves of rotational frequency of the two tubes, i.e. the tendencies of the two curves vary alternately. The two tubes in the rotor do not rotate synchronously until the CNT approaches a stable state;
(3) The relative rotational angle becomes higher over time. But finally, the two tubes in rotor rotate synchronously;
(4) When the BPNT is longer than the CNT, at higher temperature, e.g. 300 K, the BPNT is severely damaged soon after rotation. The damaged BPNT rotates synchronously with the CNT. When the two tubes are of equal length, the rotational frequency of the damaged BPNT decreases rapidly after more breakages of P–P bonds occur in the BPNT.

In the design of a nanomachine (or rotary nanomotor) with BPNT as a component, conclusion (4) above is important.

References

[1] Novoselov K S, Geim A K, Morozov S V, Jiang D, Zhang Y, Dubonos S V, Grigorieva I V and Firsov A A 2004 *Science* **306** 666–9
[2] Splendiani A, Sun L, Zhang Y, Li T, Kim J, Chim C-Y, Galli G and Wang F 2010 *Nano Lett.* **10** 1271–5
[3] Britnell L, Ribeiro R, Eckmann A, Jalil R, Belle B, Mishchenko A, Kim Y-J, Gorbachev R, Georgiou T and Morozov S 2013 *Science* **340** 1311–4
[4] Jones A M, Yu H, Ross J S, Klement P, Ghimire N J, Yan J, Mandrus D G, Yao W and Xu X 2014 *Nat. Phys.* **10** 130–4

[5] Ovchinnikov D, Allain A, Huang Y-S, Dumcenco D and Kis A 2014 *ACS Nano* **8** 8174–81
[6] Low T, Roldán R, Wang H, Xia F, Avouris P, Moreno L M and Guinea F 2014 *Phys. Rev. Lett.* **113** 106802
[7] Li L, Yu Y, Ye G J, Ge Q, Ou X, Wu H, Feng D, Chen X H and Zhang Y 2014 *Nat. Nanotechnol.* **9** 372–7
[8] Liu H, Neal A T, Zhu Z, Luo Z, Xu X, Tománek D and Ye P D 2014 *ACS Nano* **8** 4033–41
[9] Rodin A, Carvalho A and Neto A C 2014 *Phys. Rev. Lett.* **112** 176801
[10] Xia F, Wang H and Jia Y 2014 *Nat. Commun.* **5** 4458
[11] Na J, Lee Y T, Lim J A, Hwang D K, Kim G-T, Choi W K and Song Y-W 2014 *ACS Nano* **8** 11753–62
[12] Buscema M, Groenendijk D J, Steele G A, van der Zant H S and Castellanos-Gomez A 2014 *Nat. Commun.* **5** 4651
[13] Li W, Yang Y, Zhang G and Zhang Y-W 2015 *Nano Lett.* **15** 1691–7
[14] Ling X, Wang H, Huang S, Xia F and Dresselhaus M S 2015 *Proc. Natl Acad. Sci.* **112** 4523–30
[15] Rudenko A N, Brener S and Katsnelson M I 2016 Intrinsic charge carrier mobility in single-layer black phosphorus *Phys. Rev. Lett.* **116** 246401
[16] Iijima S 1991 *Nature* **354** 56–8
[17] Qiu W, Li Q, Lei Z K, Qin Q H, Deng W L and Kang Y L 2013 *Carbon* **53** 161–8
[18] Legoas S, Coluci V, Braga S, Coura P, Dantas S and Galvao D 2003 *Phys. Rev. Lett.* **90** 055504
[19] Zhang H, Cai K and Wang L 2008 *Mater. Lett.* **62** 3940–3
[20] Shulaker M M, Hills G, Patil N, Wei H, Chen H-Y, Wong H-S P and Mitra S 2013 *Nature* **501** 526–30
[21] Qiu W, Kang Y L, Lei Z K, Qin Q H, Li Q and Wang Q 2010 *J. Raman Spectrosc.* **41** 1216–20
[22] Qiu W, Kang Y, Lei Z, Qin Q H and Li Q 2009 *Chin. Phys. Lett.* **26** 080701
[23] Stankovich S, Dikin D A, Dommett G H, Kohlhaas K M, Zimney E J, Stach E A, Piner R D, Nguyen S T and Ruoff R S 2006 *Nature* **442** 282–6
[24] Balandin A A, Ghosh S, Bao W, Calizo I, Teweldebrhan D, Miao F and Lau C N 2008 *Nano Lett.* **8** 902–7
[25] Soldano C, Mahmood A and Dujardin E 2010 *Carbon* **48** 2127–50
[26] Marianetti C A and Yevick H G 2010 *Phys. Rev. Lett.* **105** 245502
[27] Seifert G and Hernandez E 2000 *Chem. Phys. Lett.* **318** 355–60
[28] Guo H, Lu N, Dai J, Wu X and Zeng X C 2014 *J. Phys. Chem.* C **118** 14051–9
[29] Jamieson J C 1963 *Science* **139** 1291–2
[30] Endo S, Akahama Y, Terada S-I and Narita S-I 1982 *Japan. J. Appl. Phys.* **21** L482
[31] Rissi E N, Soignard E, McKiernan K A, Benmore C J and Yarger J L 2012 *Solid State Commun.* **152** 390–4
[32] Qin Z, Qin Q H and Feng X Q 2008 *Phys. Lett.* A **372** 6661–6
[33] Lee C, Wei X, Kysar J W and Hone J 2008 *Science* **321** 385–8
[34] López-Polín G, Gómez-Navarro C, Parente V, Guinea F, Katsnelson M I, Pérez-Murano F and Gómez-Herrero J 2015 *Nat. Phys.* **11** 26–31
[35] Jiang J-W and Park H S 2014 *J. Phys. D: Appl. Phys.* **47** 385304
[36] Wei Q and Peng X 2014 *Appl. Phys. Lett.* **104** 251915
[37] Yang Z, Zhao J and Wei N 2015 *Appl. Phys. Lett.* **107** 023107
[38] Cai K, Wan J, Wei N, Cai H and Qin Q H 2016 *Nanotechnology* **27** 235703
[39] Cai K, Wan J, Wei N and Qin Q H 2016 *Nanotechnology* **27** 275701
[40] Fennimore A, Yuzvinsky T, Han W-Q, Fuhrer M, Cumings J and Zettl A 2003 *Nature* **424** 408–10
[41] Tu Z and Hu X 2005 *Phys. Rev.* B **72** 033404
[42] Cai K, Li Y, Qin Q H and Yin H 2014 *Nanotechnology* **25** 505701
[43] Cai K, Yu J, Yin H and Qin Q H 2015 *Nanotechnology* **26** 095702
[44] Cai K, Wan J, Qin Q H and Shi J 2016 *Nanotechnology* **27** 055706
[45] Stillinger F H and Weber T A 1985 *Phys. Rev.* B **31** 5262
[46] Jiang J-W 2015 *Nanotechnology* **26** 315706
[47] Stuart S J, Tutein A B and Harrison J A 2000 *J. Chem. Phys.* **112** 6472–86
[48] Jones J E 1924 *Proc. R. Soc.* A **106** 463–77 (The Royal Society)
[49] Nosé S 1984 *J. Chem. Phys.* **81** 511–9
[50] Plimpton S 1995 *J. Comput. Phys.* **117** 1–19
[51] LAMMPS 2016 Molecular Dynamics Simulator (http://lammps.sandia.gov/)
[52] Guo Z, Chang T, Guo X and Gao H 2011 *Phys. Rev. Lett.* **107** 105502